Analytical Methods

Accepted Manuscript

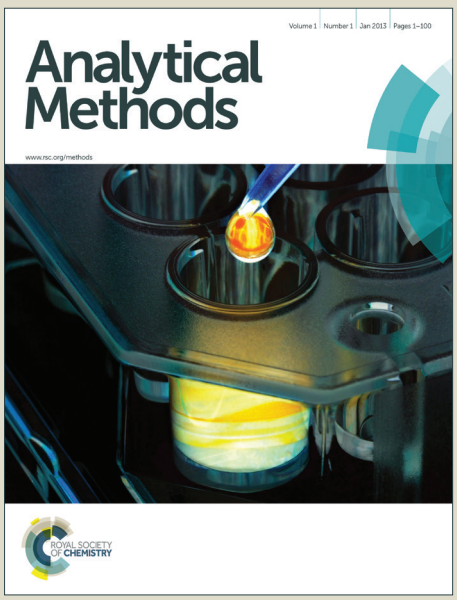

ROYAL SOCIETY OF CHEMISTRY

www.rsc.org/methods

Detection and imaging of fatty plaques on blood vessels using functionalized carbon dots

A. Shanti Krishna, C. Radhakumary[*]*, and K. Sreenivasan*[*]

Laboratory for Polymer Analysis, Bio Medical Technology Wing,

Sree Chitra Tirunal Institute for Medical Sciences and Technology,

Thiruvananthapuram-695012-India

E-mail: sreeni@sctimst.ac.in, radha.changerath@gmail.com

ABSTRACT

Risk of developing atherosclerosis is proportional to blood cholesterol level which in turn eventually leads to heart attack. Since a large number of asymptomatic young people have evidence of atherosclerosis it is highly necessary to diagnose it at the earliest. This communication depicts a simple method to visualize cholesterol deposits using digitonin (DG) conjugated carbon dots (CDs). Physico chemical characterizations and preliminary blood compatibility evaluation of the functionalized CDs (CDDG) were successfully carried out. It is found that the probes could selectively bind cholesterol as evident from their ability to image cholesterol doped polymer films and tissues with heavy fatty plaques suspended in blood serum. An early visualization of cholesterol rich plaques using fluorescent nano probes reported here may aid in diagnosis of atherosclerosis and it seems that our finding may catalyze further developments in this imperative domain. The data emerged from the study also indicate that the novel probe can be used for the selective detection of cholesterol in solution.

KEYWORDS

Atherosclerosis; Cholesterol; Digitonin; Fluorescence; Carbon Dots

INTRODUCTION

Cardiovascular disease caused over 18 million deaths in the world in 2005[1]. On the basis of Heart Disease and Stroke Statistics — 2015 update, report from the American Heart Association, cardiovascular disease remains the No. 1 global cause of death with 17.3 million deaths each year, and is expected to rise to more than 23.6 million by 2030. As per the guidelines of National Cholesterol Education Program (NCEP), elevated individual plasma cholesterol levels exceeding 6.2 mM (240 mg/dL) are indications of poor cardiovascular conditions[2]. Cholesterol, an important component of animal cell membrane[3] and an essential lipid of human body, has a major role in maintaining the integrity of biological membranes[4]. Cholesterol is delivered to the cells via the bloodstream. A comprehensive study of Cholesterol crystals in atherosclerotic plaques have been carried out by Potma et al[5]. High blood cholesterol is risky as it sticks onto the artery walls producing fatty plaques resulting in atherosclerosis[6]. Unfortunately such plaques in the initial stage evade commonly followed clinical practices. Hence, the estimation of blood cholesterol is one of the most widely performed assays in biochemistry[7]. Enzymatic analysis using auto analyzers are the commonly used standard approach for cholesterol estimation in all clinical laboratories since 1980[8-10]. However, intrinsic instability of the enzymes and subsequent loss of their activity is a serious concern on the accuracy of enzymatic detection of cholesterol [11]. Nanostructured systems are ideal platforms for the fabrication of non enzymatic cholesterol sensors and have been reported by some groups[7, 11-13]. A hybrid system tuned from β-cyclodextrin-graphene combination has recently been reported for the optical detection of cholesterol[14].

Fluorescent nano particles have received much attention in the biomedical field as diagnostics and for the investigation of molecular interactions as they are sensitive and easy to operate[15]. Among a wide variety of fluorescent nano materials, quantum dots is a forerunner for bioimaging applications. However, their toxicity and water insolubility limit their application in biomedical fields. CDs constitute a fascinating class of nanocarbons possessing several favorable attributes such as biocompatibility, chemical inertness, green synthetic route and optical stability[16-18]. Multistep design approaches can generate CDs with engineered surface features having better biocompatibility and long-term stability, demanded for a wide variety of applications[19]. The excellent photoluminescence properties of CDs make them potential candidates in sensing and imaging applications[20]. Shen et al have reported blood glucose sensing using CDs prepared using phenylboronic acid as the sole precursor [21]. Yuan et al have successfully devised a sensor based on amine coated CDs for Hg^{2+} detection [22]. Recently, CDs synthesized from starch was used for the selective detection of fluoride ions in aqueous solution[23]. Aptamer functionalized CDs for sensitive and selective detection of thrombin has been reported by Xu et al [24]. CD based probes for locating calcium rich sites in bone cracks has been reported from our group[25]. CDs for imaging human serum proteins on gels have been reported by Na et al[26]. Hyaluronic acid conjugated CDs were reported for the in vitro and in vivo real time bio imaging applications[27]. CDs as potential probes for cell imaging have recently been reported by several groups [28, 29].

Our intention here is not to quantify serum cholesterol, but to visualize cholesterol deposits using fluorescent CDs. It is still a challenge to achieve a simple, rapid and cost effective method for imaging cholesterol deposits. Sobota et al used a recombinant probe, perfringolysin O fused with glutathione S-transferase (GST-PFO) to detect cholesterol deposits in cells for the

diagnostics of Niemann-Pick disease type C (NPC), a lysosomal storage disorder caused by accumulation of unesterified cholesterol in cells of the brain and liver [30-32]. Digitonin, (DG) a glycoside obtained from Digitalis purpurea, is used in removing membrane proteins, precipitating cholesterol and permeabilizing cell membranes[33]. Digitonin is well known for its affinity towards cholesterol. A Digitonin conjugated gold nanoparticle for cholesterol sensing has been reported earlier[7]. Here in, we report the design of a novel fluorescent probe, CDs conjugated with DG for the fluorescent imaging of life threatening cholesterol deposits in biological tissues. Amino functionalized CDs were synthesized as reported earlier[34]. Synthetic route for the formation of amine capped CDs is shown in Scheme S1 (supporting information). CDs were conjugated with digitonin to form CDDG using simple chemistry as detailed in Scheme 1 and were characterized by FTIR, ^{1}H NMR, TEM, DSC, EDAX, UV-Visible spectrophotometer and Spectrofluorimeter. Zeta potential and *in vitro* heamocompatibility of the conjugate were also assessed. Binding of the probe to the cholesterol rich tissue was visualized by a hand-held UV lamp and an *in vivo* imaging system (IVIS).

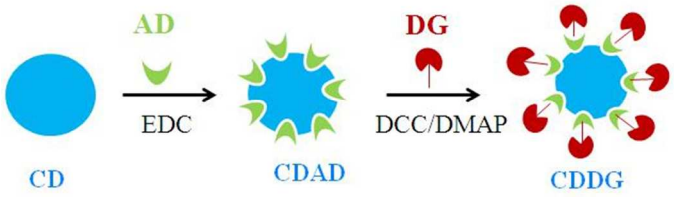

Scheme 1. Modification of CDs with digitonin. CD is first anchored with adipic acid (AD) and then DG is conjugated using DCC/DMAP

EXPERIMENTAL SECTION

Materials

Citric acid anhydrate, Poly(ethylene glycol) bis(3-aminopropyl) terminated (MW 1500), Glycerine, Adipic acid (AD), N-(3-Dimethylaminopropyl)-N'ethylcarbodiimide (EDC), Digitonin, Dicyclohexylcarbodimide (DCC), Dimethylamino pyridine (DMAP), Cholesterol, Valine, Cystine, Glycine, Lysine, Tryptophan, Methionine, ascorbic acid, dopamine, glutathione and uric acid were obtained from sigma Aldrich, Bangalore. All other chemicals used were of analytical grade and obtained from Merck India Ltd, Mumbai, India.

Synthesis of amino functionalized CDs

These probes were synthesized as reported earlier [34]. In brief, 9 mL of glycerin and 600 mg of PEG diamine were taken in a 100 mL three-neck flask and degassed with nitrogen for 10 min. As the temperature reaches to 250 °C, 600 mg of citric acid was quickly added, allowed to react at this temperature for 3 h and then cooled down to room temperature. The resulting product was dialyzed against distilled water using a cellulose ester dialysis membrane [molecular weight cut off (MWCO) = 3500] for 2 days in order to remove any unreacted reactants.

Conjugation of DG onto CDs. Amine capped CDs were modified with adipic acid (AD) via EDC chemistry to get carboxyl terminated CDs. CDs were mixed with 0.013 M AD and 20 fold molar excess of EDC after adjusting the pH to ~ 4.2. The reaction mixture was kept overnight at 4°C and the resulting solution was purified by dialyzing against distilled water using a cellulose ester dialysis membrane [MWCO = 3500] for 2 days in order to remove any unreacted reactants. Further, 0.013 M digitonin was conjugated onto CDAD in presence of DCC/DMAP at room temperature, overnight and the resulting solution was dialyzed against DMSO/H_2O mixture using a cellulose ester dialysis membrane [MWCO = 3500].

Characterization techniques

Fourier Transform Infra Red (FTIR) spectra of CD, CDAD and CDDG were collected in the range 600-4000 cm^{-1} on a Nicolet 5700 FTIR Spectrometer, Nicolet Inc, Madison, USA using a Diamond ATR accessory. Proton Nuclear Magnetic Resonance (^1H NMR) spectra of CDDG and digitonin were recorded using 500 MHz Bruker AV 500 NMR spectrometer, Switzerland.

High Resolution Transmission electron microscopy (HRTEM) was performed in an FEI, TECNAI S Twin microscopy (Netherland) with an accelerating voltage of 100 KV. The sample solutions (CD) were prepared by dispersion under an ultrasonic vibrator. They were then deposited on a formvar coated copper grid and dried in a vacuum at room temperature before observation.

Transmissions Electron Microscopic (TEM) images of CDDG were obtained on a Hitachi, H 7650 microscope, Hitachi, Tokyo, Japan. The colloidal solution (CDDG) was deposited onto a 200 mesh copper grid coated with a formvar film and dried overnight.

Zeta potential values of CD, CDAD and CDDG were determined using Dynamic Light Scattering (DLS) (Malvern Instruments Ltd, UK).

Energy dispersive X-ray analysis (EDAX) of CDs was carried out. (ESEM-EDS Quanta 200, The Netherlands). Oxford X-ray microanalysis software was used for data processing. Line mapping was done in three fields to know the distribution of the elements in the sample.

UV-Visible absorption spectrum was taken using a UV-Visible spectrophotometer (Varian, Cary 100 Bio, Melbourne, Australia).

The fluorescence intensity of the same were measured using a Varian, Cary Eclipse model EL 0507 Spectrofluorimeter (Melbourne, Australia).

Thermal analysis was carried out with Differential scanning calorimeter (DSC), TA Instruments (USA), DSC Q100, using MDSC (Modulated DSC) mode under nitrogen atmosphere at a heating rate of 3 ºC min^{-1} and at a modulation amplitude of 1ºC for a period of 60 s.

The fluorescent images were taken using a Fluorescent microscope, Leica DM IL Generic, Switzerland.

Xenogen (Caliper Life Sciences) IVIS Spectrum *in vivo* imaging system (USA) was used to visualize the binding of the probe onto the fatty deposits of tissues.

In vitro hemocompatibility of the material

Blood from human volunteer was collected into the anticoagulant ACD. Each sample was transferred to polystyrene petri dishes and 2 mL blood was added, 1 mL blood was taken immediately for initial analysis and remaining 1 mL blood was incubated with samples for 30 min under agitation at 70 ± 5 rpm using an Environ shaker thermo stated at 35 ± 2 ºC. Four empty polystyrene culture dishes were exposed with blood as reference. The total hemoglobin in the whole blood samples were measured using automatic Hematology Analyzer (Sysmex-K 4500). The free hemoglobin liberated into the plasma after exposure to samples were measured using diode array spectrophotometer and the percentage hemolysis was calculated using the formula, (Free Hb/Total Hb/1000) x 100.

Biological specimens

Fat tissue (with atherosclerotic deposit) and tissue without deposit were extracted from blood vessels surrounding the human heart tissue collected during autopsy. Consent was taken for collecting heart valve for homograft banking as per the ethical guidelines of our Institute.

RESULTS AND DISCUSSION

FTIR spectrum (Figure S1) shows peaks at 1637 cm^{-1} and 1558 cm^{-1} corresponding to –CO- stretching and –NH- bending vibrations respectively confirming the formation of CD amended with adipic acid (CDAD). On conjugation of DG a strong peak appears at 1011 cm^{-1}, characteristic of C-O-C group, substantiating the ester bond formation between CDAD and DG to form CDDG. This is further supported by the ^{1}H NMR spectra (Figure S2). In Figure S2A, the peak at 3.6 ppm for CDDG is attributed to the methylene group of PEG diamine used for the synthesis of CD. Those peaks at 2.6 ppm and 1.2 ppm correspond to the methylene groups and aliphatic hydrogen atoms respectively of the DG moiety. These peaks assignment are ascertained by comparing the spectrum of DG alone (Figure S2B).

CDs are expected to be formed due to the pyrolysis of citric acid with PEG diamine as the capping agent. To get a view whether, NH2 groups are present on the generated CDs, EDAX analysis was carried out (Figure S3). Data generated from EDAX analysis showed the wt% of the elements Carbon, Nitrogen and Oxygen as 56.36 %, 14.42 % and 29.22 % respectively. The presence of Nitrogen thereby confirms CDs contain amine as the end groups. In the EDAX trace, however, peak associated with N2 is overlapped with the predominant carbon peak and cannot be observed as a distinct peak. The peak at 3436 cm^{-1} in the FTIR spectrum (Figure S1) of CD indicates the presence of NH_2 groups confirming the capping of PEG diamine. A peak at δ= 3.6 ppm attributable to the methylene group of PEG diamine further confirms coverage of the formed CDs by amino groups.

CDs possess spherical morphology and have an average size of 4 nm (Figure 1A). TEM image (Figure 1B) of CDDG indicates that the size has increased to ~10 nm on conjugation. Modification may result in the interaction among functional groups leading to the formation of aggregates and thereby an increase in size. Similar observation has been reported earlier

also[25,35,36]. Zeta potential values (Table S1, supporting information) denote that the negative charge on CD (-20.90 mV) is reduced to -6.78 mV and -4.99 mV on formation of CDAD and CDDG respectively. The overall reduction of negative charge could be attributed to the integration of DG which is relatively hydrophobic.

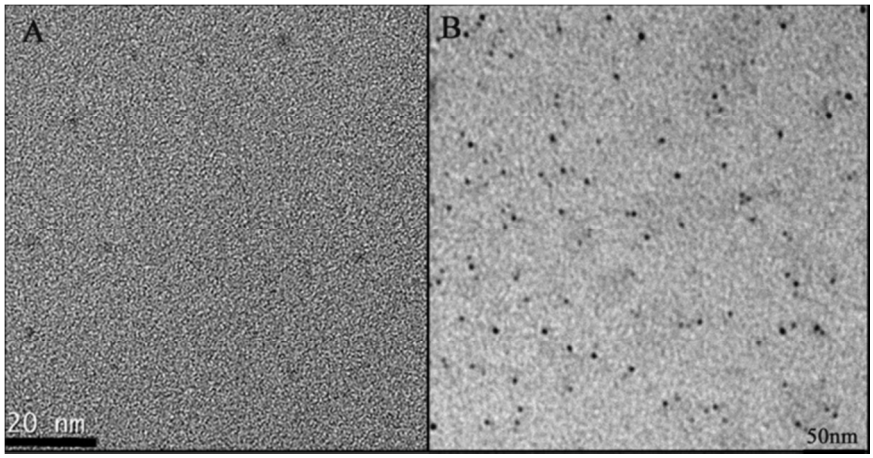

Figure 1. A) HRTEM micrograph of CDs B) TEM micrograph of CDDG

UV-Visible absorption spectrum of CDDG (Figure S4A) shows absorption maximum at 360 nm. Fluorescence excitation and emission spectra of CDDG given in Figure S4B (supporting information) show an emission peak maximum of 455 nm on excitation at 360 nm. Fluorescence emission spectra of CD, CDAD and CDDG are shown in Figure 2. There is no shift in the peak maximum after conjugation but an increase in the fluorescence intensity of CDDG was observed comparing to CD which could be due to the enhanced hydrophobic environment resulted by incorporation of DG moieties. The photographic images of CD (A), CDAD (B) and CDDG (C) in day light and UV light are given in the inset of Figure 2. The blue fluorescence under UV lamp at 365 nm for CDAD and CDDG ensure that the conjugation does not affect the fluorescent property of CD.

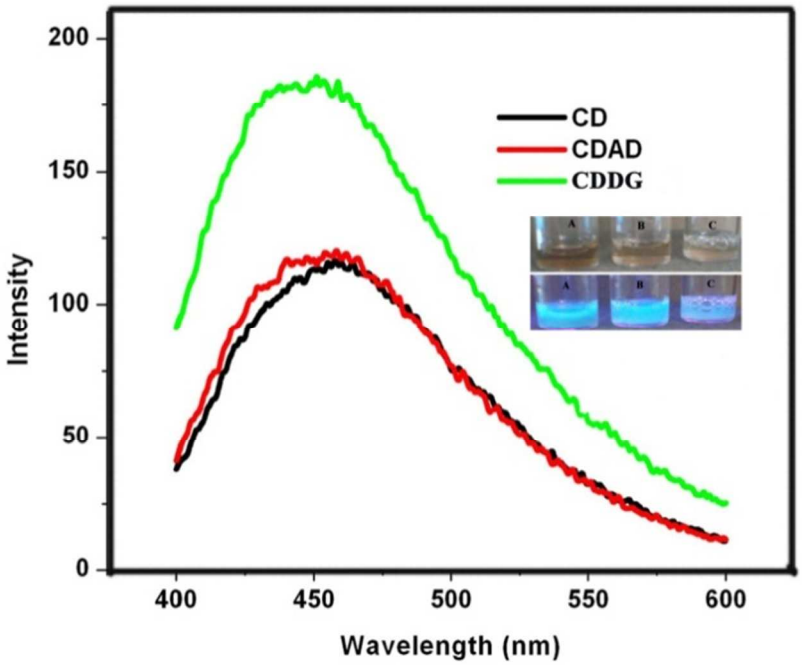

Figure 2. Fluorescence emission spectra of A) CD, B) CDAD and C) CDDG. Inset shows the photograpic images of corresponding solutions in day light and under UV (365 nm)

The variation in fluorescence intensity of the probe, CDDG with varied concentrations of cholesterol (2 mM - 20 mM) is given in Figure S5. 2 mL of CDDG (0.06 mg/mL) solutions were taken in different tubes and 200 µL of cholesterol solutions (2 mM - 20 mM) were added into each. The solutions were mixed thoroughly and their fluorescence spectra were recorded. It was observed that the fluorescence intensity decreased with increasing concentrations of cholesterol which may be due the surface quenching states induced mechanism which has been mentioned for the fluorescence quenching in some of the earlier reports[21, 37]. As given in the introduction, the elevated individual plasma cholesterol levels exceeding 6.2 mM (240 mg/dL) are indications of poor cardiovascular conditions. Hence the cholesterol concentration range 2 mM - 20 mM was chosen to study the change in the fluorescence intensity of CDDG. Linearity between the relative fluorescence intensities of CDDG and various cholesterol concentrations with correlation coefficient of 0.987 was obtained as given in Figure S6. F0 and F are the fluorescence intensities

of CDDG in the absence and presence of cholesterol respectively. Effective fluorescence quenching was observed for lower concentrations of cholesterol i. e. 2 mM (77 mg/dL) and 4 mM (155 mg/dL) which is far below the cholesterol level (> 6.2 mM) responsible for cardiovascular diseases. Thus the detection limit was found to be 2 mM though the estimation or quantification of cholesterol is not the objective of our approach.

Selectivity of the probe for binding cholesterol was confirmed by studying the interaction with other steroids like testosterone, hydrocortisone and corticosterone. The interference of CDDG in presence of 20 mM of testosterone, hydrocortisone and corticosterone was checked. 2 mL of CDDG (0.06 mg/mL) solutions were taken in different tubes and 200 µL of these steroids were added into each. The solutions were mixed thoroughly and their fluorescence spectra were recorded. Figure S7 depicts that the fluorescence intensity of CDDG remained unaffected in presence of other steroids thus proving the binding of the probe to cholesterol. The response of CDDG to potential coexisting substances in serum, including some amino acids [valine (val), Cystine (cys), Glycine (gly), Lysine (lys), Tryptophan (trypt) and Methionine (meth)] ascorbic acid (aa), dopamine (dop), glutathione (gt) and uric acid (ua) was also studied. 100 µM concentrations of all these biomolecules were prepared and 200 µL of these were added to 2 mL of CDDG (0.06 mg/mL) solutions were taken in different tubes. The solutions were mixed well and their fluorescence spectra were recorded. It was observed that these molecules did not quench the fluorescence intensity of CDDG significantly when compared with CDDG incubated with 15 mM of cholesterol as given in the Figure S8.

A preliminary experiment as given below was done to confirm that CDDG can bind cholesterol. 50 µL of sigma grade cholesterol solution (10 mM, DMSO-water mixture) was sprayed onto glass cover slip, air dried and incubated with aqueous CDDG (0.06 mg/mL).

After 1 h, the surface was washed and viewed under a fluorescence microscope at 20X using various filters. It can be seen that in all the three images (Figure S9) cholesterol rich areas on the glass slides are fluorescent and the empty areas are dark in colour confirming that the CDDG has high affinity towards cholesterol. Further, the same experiment was repeated with Poly Vinyl Alcohol (PVA) films both bare and doped with cholesterol. It can be seen in Figure 3 that the cholesterol doped area specifically fluoresce leaving the other part dark.

Figure 3. Fluorescence microscope images of cholesterol doped on PVA film, incubated with CDDG and viwed under different filters.

The blue, green and red fluorescence obtained (in figure S9 and figure 3) using various filters [UV range (350-380 nm), blue (450-490 nm) and green (515-560 nm) respectively] show that CDDG exhibit excitation dependent fluorescence property. It is a known fact that CDs exhibit different emissions depending on excitation wavelengths[27] which is also shown by CDDG as given in Figure S10. These types of varied optical features attribute to the size distribution of CD or emission trap distribution on CD surfaces[38-40]. Photoluminescence dependent excitations exhibited by CDs when coated on paper, animal fur or skin have been reported[41].

The fluorescence intensity of the residual solution after removing the PVA films was also measured (Figure S11) and found to be very less for the solution in which cholesterol doped

PVA film was incubated. The intensity of the same was significantly high in which bare PVA film was immersed; clearly indicating that CDDG has high affinity towards cholesterol.

As already proved (Figure 2) and further demonstrated by the above experiments, the functionalization of CD with digitonin did not affect the fluorescence property of CDs and could be used as promising cholesterol targeting and imaging nano probes.

Percentage haemolysis for CDDG (0.06 mg/mL) is 1.7%. According to the E2524-08 protocol, if the percentage hemolysis for a test-nanomaterial is equal to or less than 2 %, the material is considered as non-hemolytic [42,43].

Finally, we repeated the experiment using a piece of tissue with heavy fat deposit extracted from the blood vessels that surround the human heart. We conducted Modulated Differential Scanning Calorimetry (MDSC) analysis of the deposit collected from the tissue as detailed in the experimental section. MDSC analysis was also carried out using fatty deposit free tissue to compare the phase transitions as depicted in Figure S12. Melting point of pure cholesterol is 148 ºC as per literature. The fat tissue showed a prominent melting peak at 102 ºC. We presumed that this peak is associated with lipids predominantly cholesterol. The reduction in melting peak may be explained by the fact that the deposit contains apart from cholesterol, other entities like cholesterol esters and lipids in various proportions. No such transition is shown by the muscle tissue as indicated in the trace (Figure. S12).

The fat deposited tissue was incubated with CDDG solution for various time intervals i.e. 5 min, 30 min, 1 h, 2 h and 24 h. Subsequently, they were taken out, washed with water and viewed

under UV lamp at 365 nm. Images shown in Figure 4 demonstrate that even after 5 min the tissue shows fluorescence. On the other hand it can be seen in Figure 5 that the muscle portion of the tissue (with no fat deposit) did not fluoresce at all when underwent the same steps.

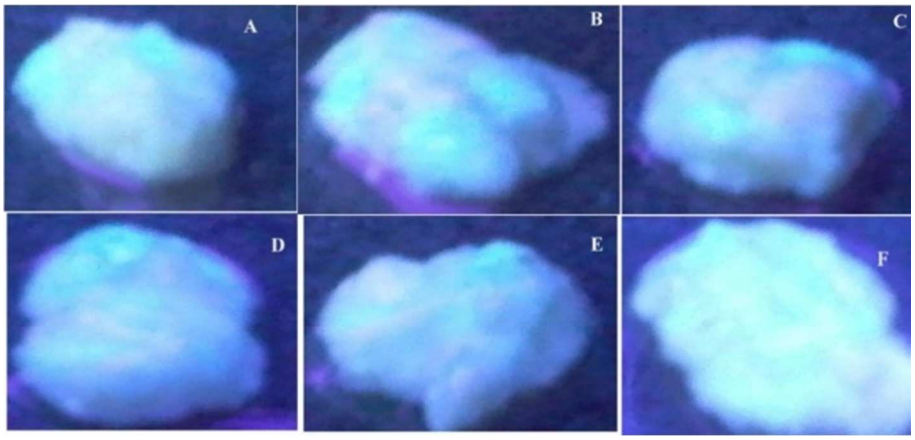

Figure 4. Fat tissue incubated with CDDG for varied time intervals and viwed under UV lamp A) 5 min B) 15 min C) 30 min D) 1 h E) 2 h F) 24 h. The ability of the probe to bind rapidly onto cholesterol rich spot is apparent from these images.

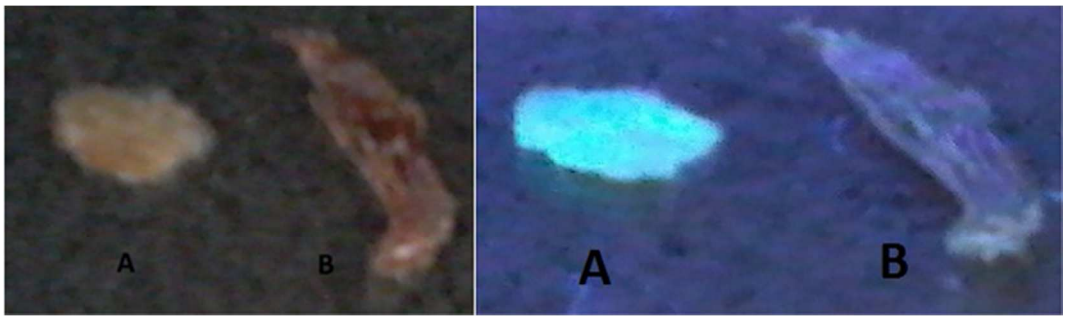

Figure 5. A) Fat tissue B) Muscle tissue incubated with CDDG for 24 h, when viewed in day light (left) and under UV lamp at 365 nm (right)

Further, to mimic the actual *in vivo* condition, the fat deposited tissue and the deposit free tissue were incubated with blood serum containing 230 mg/dL cholesterol (Human blood collected from one of the authors) mixed with the probe (CDDG) and kept at 37 ºC under shaking for 1 h .The tissues were then washed and viewed under UV lamp at 365 nm. This experiment was performed to get an insight into the probe's behavior in a medium which already contains

cholesterol in free and bound forms. Under such a situation, the probe need not bind onto the cholesterol deposit instead it can bind to the cholesterol present in the medium. Surprisingly, it can be seen in Figure 6 that the fat deposited tissue shows fluorescence while fat free tissue is non fluorescent confirming that the probe can recognize and dock onto the fat deposits in real situation (*in vivo*).

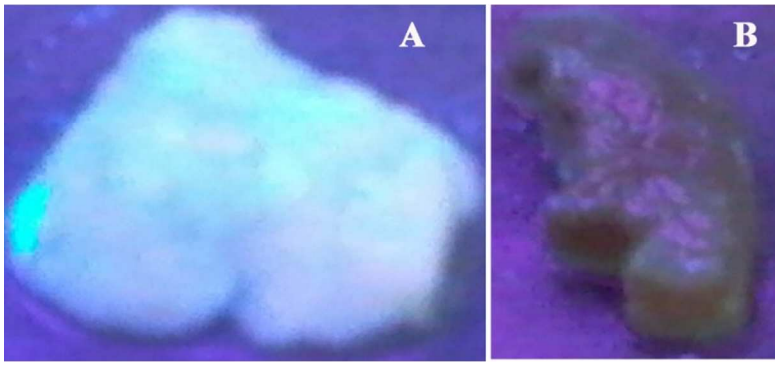

Figure 6. A) Fat tissue and B) Fat free tissue incubated with CDDG in blood serum, under UV light at 365 nm. Only fat deposited tissue (Fig. A) shows fluorescence.

The tissues were also imaged with Xenogen (Caliper Life Sciences) IVIS Spectrum *in vivo* imaging system at an excitation wavelength of 430 nm (the starting wavelength available for the equipment). From Figure 7 it is clear that the fat tissue (left) has maximum binding of the probe as evident from the color bar. The red region indicates maximum fluorescence intensity and blue the minimum. It is obvious that the fat deposit free tissue is completely blue in color confirming that the probe has not bound to it at all. This experiment further supports the ability of CDDG as a fatty deposit plaque imaging probe.

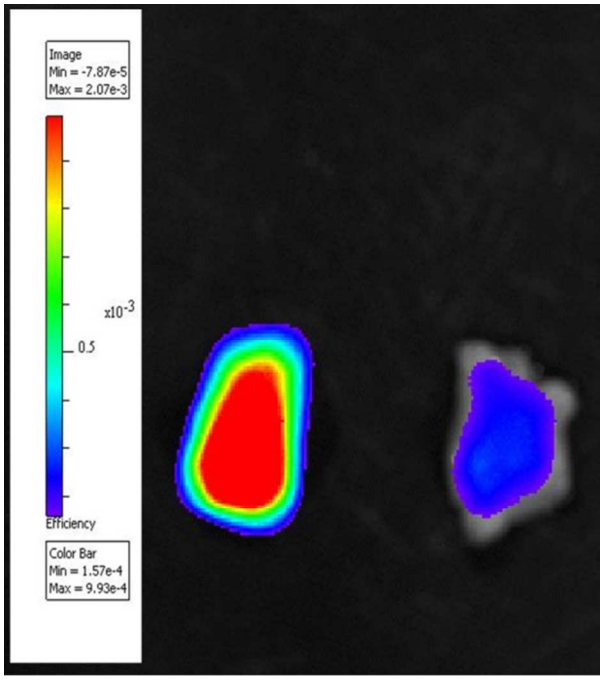

Figure 7. Fat Tissue (left) and muscle tissue (right) imaged with the IVIS system

CONCLUSIONS

In summary, digitonin conjugated carbon dot based nanoprobe for imaging cholesterol deposits was successfully synthesized and characterized. The probes could bind onto the cholesterol rich areas as evident from fluorescent microscope and IVIS Spectrum images. The probe can be thus used for the early detection of plaque formation, saving the lives of many asymptomatic atherosclerotic patients especially youngsters. We feel that the simple methodology portrayed here has significant promise for *in vivo* imaging. The data also indicate that the novel probe could be used for the selective detection of cholesterol in solution.

ACKNOWLEDGEMENTS

Authors wish to thank DBT, New Delhi for funding. Authors are also grateful to Ms. S. Many, TEM lab for the TEM images, Ms Priya, DPL, for zeta potential, Ms. Rakhi, DTERT lab for her technical assistance in getting fluorescent images, Biophotonics laboratory, SCTIMST for IVIS Spectrum *invivo* imaging system and NIIST, Trivandrum for ^{1}H NMR and HRTEM facilities.

REFERENCES

1. Strong, K.; Mathers, C.; Leeder, S.; Beaglehole, R. *Lancet.* **2005**, *366*, 1578-82.
2. Nauck, M.; Marz, W.; Wieland, H. *Clin. Chem*. **2000**, *46*, 436–437.
3. Ikonen, E. *Nat. Rev. Mol. Cell Biol*. **2008**, *9*, 125–138.
4. Radwan, A.A; Alanazi, F.K. *Saudi Pharm J.* **2014,** *22*, 3–16.
5. Suhalim, J. L; Chung, C.Y; Lilledahl, M.B; Lim, R.S; Levi, M; Tromberg, B.J; Potma, E.O. *BiophysJ*. **2012**, *102*, 1988-95.
6. Raines, W. E.; Ross, R. *J. Nutr***. 1995**, *125*, 624S–630S.
7. Raj, V.; Jaime, R.; Astruc, D.; Sreenivasan, K. *Biosens. Bioelectron*. **2011,** *27*, 197-200.
8. Bergmeyer, H.; Grassl, M. 3rd edition, Wiley-VCH, Weinheim, 1990
9. Richmond. W. *Anal. Clin. Biochem.* **1992,** *29*, 577-597
10. Pasin, G.; Smith, G.M.; Machony, M.O. *Food. Chem*. **1998**, *61*, 255-259
11. Raj, V.; Johnson, T.; Joseph, K. *Biosens Bioelectron*. **2014**, *60*, 191-4.
12. Li, Y.; Bai, H.; Liu, Q.; Bao, J.; Han, M.; Dai, Z. *Biosens Bioelectron*. **2010**, *25*, 2356-60
13. Lee, Y.J.; Park, J.Y. *Biosens Bioelectron*. **2010**, *26*, 1353-8.
14. Mondal, A.; Jana, N. R. *Chem. Commun***, 2012***, 48*, 7316–7318.
15. Jun, M.E.; Roy, B.; Ahn, K.H. *Chem. Commun*. **2011**, *47*, 7583–7601.
16. Liu, R.; Wu, D.; Liu, S.; Koynov, K.; Knoll, W.; Li, Q. *Angew Chem Int Ed*. **2009,** *48,* 4598 –4601;
17. Baker, S. N.; Baker, G. A. *Angew. Chem*. **2010**, *122*, 6876-6881.
18. Ko, H. Y.; Chang, Y. W.; Paramasivam, G.; Jeong, M. S.; Cho, S.; Kim, S. *Chem.Commun.* **2013***, 49,* 10290—10292.
19. Ding, C.; Zhu, A.; Tian, Y. *Acc. Chem. Res*. **2014**, *47*, 20–30
20. Wen, J.; Xu, Y.; Li, H.; Lu, A.; Sun, S. *Chem Commun*. **2015**, *51*, 11346-58
21. Shen, P.; Xia, Y. *Anal. Chem*. **2014**, *86*, 5323−5329

22. Yuan, C.; Liu, B. H.; Liu, F.; Han, M. Y.; Zhang, Z. P. *Anal. Chem*. **2014**, *86*, 1123–1130.
23. Basu, A.; Suryawanshi, A.; Kumawat, B.; Dandia, A.; Guin, D.; Ogale, S.B. *Analyst*,. **2015**, *140*, 1837–1841
24. Xu, B.; Zhao, C.; Wei, W.; Ren, J.; Miyoshi, D.; Sugimoto, N.; Qu, X. *Analyst*. **2012**, *137*, 5483–5486
25. Shanti Krishna, A.; Radhakumary, C.; Sreenivasan, K. *Analyst* .**2013,** *138*, 7107–7111.
26. Na, N.; Liu, T. T.; Xu, S. H.; Zhang, Y.D.; He, C. L.; Huang, Y.; Jin, O. Y. J. Mater. Chem. B. **2013**, *1*, 787–792
27. Goh, E.J., Kim, K.S., Kim, Y.R., Jung, H.S., Beack, S., Kong, W.H., Scarcelli, G., Yun, S.H., Hahn, S.K. Biomacromolecules. **2012**, *13*, 2554–2561
28. Chen, B. S.; Li, F. M.; Li, S. X. ; Weng, W.; Guo, H. X.; Guo, T.; Zhang, X.Y.; Chen, Y.B.; Huang, T. T.; Hong, X.L.; You, S.Y.; Lin, Y.M.; Zeng, K.H.; Chen,S. *Nanoscale*. **2013**, *5*, 1967–1971
29. Zhu, X. H.; Wang, H. Y.; Jiao, Q. F.; X. Xiao, X. X. Zuo, Y. Liang, J. M. Nan, J. F. Wang and L. S. Wang. *Part. Part. Syst. Charact*. **2014**, *31*, 771–777
30. Kwiatkowska, K.; Marszałek-Sadowska, E.; Traczyk, G.; Koprowski, P.; Musielak, M.; Lugowska, A.; Kulma, M.; Grzelczyk, A.; Sobota. A. *Orphanet J Rare Dis*. **2014**, *64*, doi: 10.1186/1750-1172-9-64 Reid,
31. Reid, P.C.; Sugii, S.; Chang, T.Y. *J Lipid Res*. **2003**, *44*, 1010-9.
32. Vanier, M.T.; Millat, G. *Clin Genet*. **2003**, *64*, 269-81.
33. Nishikawa, M.; Nojima, S.; Akiyama, T.; Sankawa, U.; Inoue, K. *J Biochem.* **1984**, *96*. 1231-9.
34. Wang, F. ; Pang, S.; Wang, L. ; Li, Q.; Kreiter, M.; Liu, C. *Chem. Mater.* **2010**, *22*, 4528–4530.
35. Shanti Krishna, A.; Radhakumary, C.; Molly Antony, Sreenivasan, K. *J. Mater. Chem. B.* **2014**, *2*, 8626–8632

36. Ye, Z.; Tang, R.; Wu, H.; Wang, B.; Tan, M.; Yuana, J. *New J. Chem.* **2014,** *38,* 5721-5726

37. Wu, W.; Zhou, T.; Berliner, A.; Banerjee, P.; Zhou, S. *Angew. Chem., Int. Ed*. **2010**, *49*, 6554−6558.

38. Zhu, H.; Wang, X.; Li, Y.; Wang, Z.; Yang, F.; Yang, X. *Chem. Commun.* **2009,** *34*, 5118−5120.

39. Mochalin, V. N. Gogotsi, Y. *J. Am. Chem. Soc*. **2009**, *131*, 4594–4595.

40. Tang, L.; Ji, R.; Cao, X.; Lin, J.; Jiang, H.; Li, X.; Teng, K. S.; Luk, C. M. ; Zeng, S.; Hao , J.; Lau, S. P. *ACS Nano*, **2012**, *6*, 5102–5110.

41. Qu, S.; Wang, X.; Lu, Q.; Liu, X.; Wang, L. *Angew. Chem. Int. Ed.* **2012**, *51*, 12215 – 12218.

42. A.I.SM. E2425, Standard Test Method for Analysis of Hemolytic Properties of Nanoparticles ASTM International, **2008**

43. Dobrovolskaia, M. A.; McNeil, S.E. *J Control Release***, 2013**, *172*, 456-66.

TOC

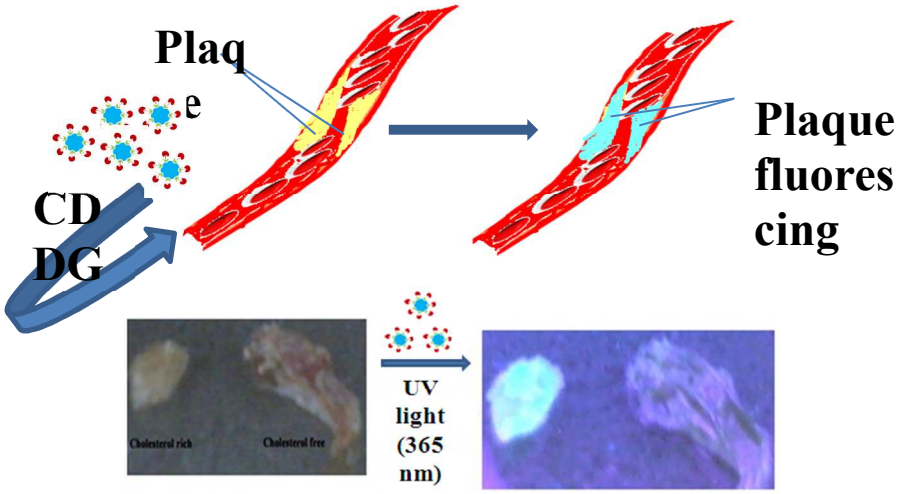

Lighting the killer deposit on arterial walls: Digitonin conjugated carbon dots enable the fluorescent imaging of cholesterol deposit in biological tissues.